1st International Conference on Mathematical and Computational Biomedical Engineering - CMBE2009
June 29 - July 1, 2009, Swansea, UK
P.Nithiarasu and R.Löhner (Eds.)

Mammographic Image Segmentation using Edge Based Deformable Contour Models

Xianghua Xie
Department of Computer Science, University of Swansea, Swansea, UK
x.xie@swansea.ac.uk

ABSTRACT

Deformable contour models, also known as snakes, are commonly used in image processing and computer vision due to their natural handling of shape variation and independence of operation (once initialized), which make them highly appropriate to segment mass lesions in digital (or digitized) mammographic images. The extracted shape and texture information through contour based segmentation are useful in determining benignancy or malignancy. In this paper, we present a preliminary sudy on comparative analysis of four edge based active contour models in segmenting mass lesions in mammogram images. Two of them are widely used, classic active contour models and the other two are most recent advances in active contouring. Experiments are carried out to compare their accuracy, as well as the ability in handling weak edges and difficult initializations.

Key Words: *Digital mammography, computer-aided diagnosis, lesion segmentation, mass segmentation, active contours, deformable model, object segmentation.*

1 INTRODUCTION

Breast cancer is one of the leading cause of cancer deaths in women and the risk of developing breast cancer in life time for women is very high, from eight to twelve percent [14]. Mammography has been proved effective in examining abnormalities for early detection which is the key to improve breast cancer prognosis. Analyzing mammogram using computer vision has been widely reported in the literature, e.g. [4, 10, 8]. Segmenting mass lesions is a critical step in automatic or computed aided detecting abnormalities and diagnosis. Masses are space occupying lesions, characterized by their shape, margin and density. A benign neoplasm is smoothly marginated, while a malignancy often has an indistinct border with low contrast which appears more spiculated over time. Some example mass lesions are shown in Figs. 1 and 2. Potential lesion sites can be automatically or semi-automatically detected and located, e.g. [4]. These regions will be closely examined. Thus lesion segmentation is useful to delineate them from surrounding tissues. Various techniques have been developed to carry out this task, including Markov random field modeling [6], region growing [2], SOM [5], fuzzy sets [9], morphological process [3], and watershed segmentation [10].

Active contour models are highly appropriate to segment mass lesions in mammographic images, e.g. [11]. In this paper, we present a preliminary study on comparative analysis of four edge based active contour models in segmenting mass lesions in mammogram images. Two of them are widely used, classic active contour models and the other two are most recent advances in active contouring. Experiments are carried out to compare their segmentation accuracy, as well as the ability in handling weak edges and difficult initializations.

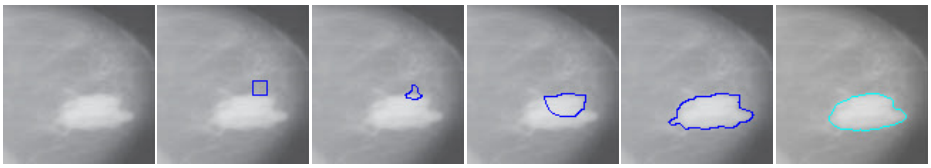

Figure 1: Mass lesion segmentation - from left: mass lesion image, initial MAC snake, its evolution, MAC final result, and the hand labeled segmentation. None of the other methods can achieve reasonable results with such difficult initialization.

2 EDGE BASED ACTIVE CONTOURING

We conduct an applied comparative study of four edge based active contour models, namely geodesic [1], GGVF [13], GeoGGVF [7] and MAC [12], in mammogram mass lesion segmentation. Due to lack of space, we only provide an overview of the more recent MAC model. Interested readers can refer to the references for more details.

The MAC model [12] is one of the most recent advances in edge based active contouring. It has shown significant improvements over other edge based models and comparable performances against more sophisticated region based methods. It is based on hypothesized magnetic interactions between the object boundary and the active contour. We hypothesize charged particles flowing through the edges. These flows of charges will then generate a magnetic field. The snake, carrying similar flow of charges, will be attracted towards the edges under this magnetic influence. Without losing generality, let us consider the image plane as a 2D plane in a 3D space whose origin coincides with the origin of the image coordinates. Additionally, the third dimension of this 3D space is considered perpendicular to the image plane.

The direction of the currents, flows of charges, running through object boundary can be estimated based on edge orientation, which can be conveniently obtained by a 90° rotation in the image plane of the normalized gradient vectors $(\hat{I}_x, \hat{I}_y)$, where I denotes an image. Let $\mathbf{x}$ denote point in the image domain. Thus, the object boundary current direction, $\mathbf{O}(\mathbf{x})$, can be estimated as: $\mathbf{O}(\mathbf{x}) = (-1)^\lambda(-\hat{I}_y(\mathbf{x}), \hat{I}_x(\mathbf{x}), 0)$, where $\lambda = 1$ gives an anti-clockwise rotation in the image coordinates, and $\lambda = 2$ provides a clockwise rotation. Since the snake is embedded in a signed distance function, the direction of current for the snake, denoted as $\boldsymbol{\Upsilon}$, can be similarly obtained by rotating the gradient vector $\nabla\Phi$ of the level set function.

Let $f(\mathbf{x})$ be the magnitude of edge pixel and the magnitude of boundary current be proportional to edge strength, that is, the electric current on object boundary is defined as $f(\mathbf{x})\mathbf{O}(\mathbf{x})$. The magnetic flux $\mathbf{B}(\mathbf{x})$ generated by gradient vectors at each pixel position $\mathbf{x}$ can then be computed as: $\mathbf{B}(\mathbf{x}) \propto \sum_{\mathbf{s}\in\mathbf{S}} f(\mathbf{s})\mathbf{O}(\mathbf{s}) \times \frac{\hat{\mathbf{R}}_{\mathbf{xs}}}{R^2_{\mathbf{xs}}}$, where $\mathbf{s}$ denotes an edge pixel position, $\mathbf{S}$ is the set containing all the edge pixel positions, $\hat{\mathbf{R}}_{\mathbf{xs}}$ denotes a 3D unit vector from $\mathbf{x}$ to $\mathbf{s}$ in the image plane, and $R_{\mathbf{xs}}$ is the distance between them. The snake is assigned with unit magnitude of electric current. The force imposed on it can be derived as: $\mathbf{F}(\mathbf{x}) \propto \boldsymbol{\Upsilon}(\mathbf{x}) \times \mathbf{B}(\mathbf{x})$. We can see that $\mathbf{B}$ intersects the image plane perpendicularly and $\mathbf{F}$ is always perpendicular to both $\boldsymbol{\Upsilon}$ and $\mathbf{B}$. Thus, $\mathbf{F}$ also lies in the image domain and its third element equals to zero. For simplicity, we shall ignore its third dimensional component and denote $\mathbf{F}(\mathbf{x})$ as a 2D vector field in the image domain. The basic MAC model can then be formulated as: $C_t = \alpha g(\mathbf{x})\kappa\hat{\mathbf{N}} + (1-\alpha)(\mathbf{F}(\mathbf{x}) \cdot \hat{\mathbf{N}})\hat{\mathbf{N}}$, where $g(\mathbf{x}) = 1/(1+f(\mathbf{x}))$, κ denotes the curvature, and $\hat{\mathbf{N}}$ is inward unit normal. Its level set representation then takes this form: $\Phi_t = \alpha g(\mathbf{x})\nabla \cdot \left(\frac{\nabla\Phi}{|\nabla\Phi|}\right)|\nabla\Phi| - (1-\alpha)\mathbf{F}(\mathbf{x}) \cdot \nabla\Phi$. Nonlinear diffusion of the magnetic field can be applied in order to overcome noise interference if necessary. More details can be found in [12].

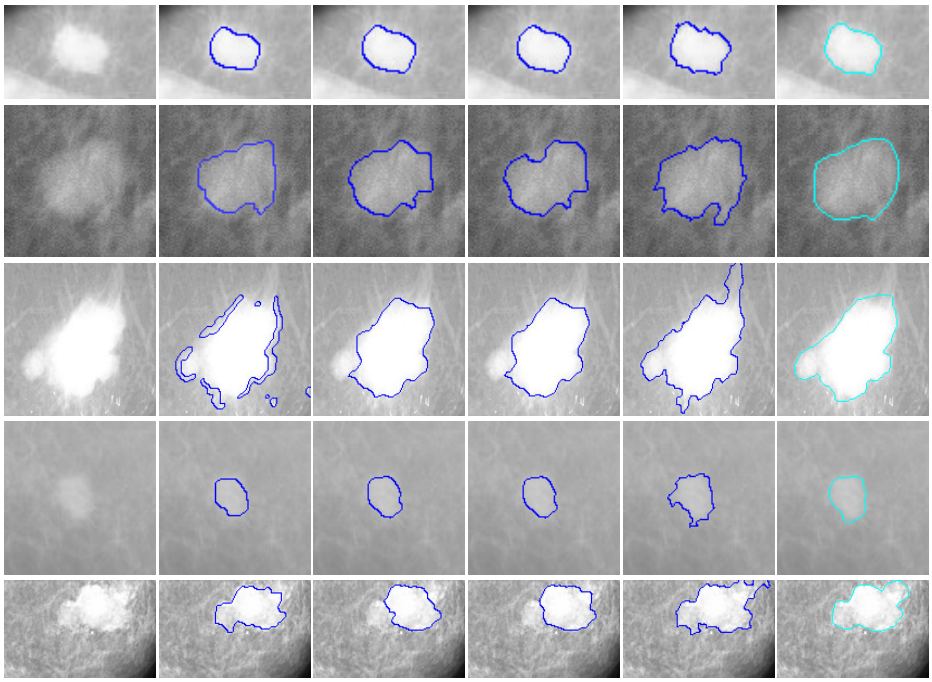

Figure 2: Mass lesion segmentation - Row (a): original mass lesion images row (b): geodesic results; row (c): GGVF results; row (d): GeoGGVF results; row (e): MAC results; row (f): hand labeled segmentations. Note the initialization conditions for the MAC model are much more challenging than those for the rest models.

Table 1: Segmentation Comparison.

Test No.		1	2	3	4	5	6	7	8	**Overall**
Geodesic	spec.	100	99.98	4.04	99.96	0	99.96	0.02	99.63	62.95
	sens.	76.40	70.75	91.25	79.65	93.14	75.72	94.38	81.25	82.82
	accu.	96.34	97.35	28.52	95.02	3.14	98.56	7.68	96.23	65.36
GGVF	spec.	100	99.98	99.19	99.84	100	99.97	99.89	99.38	99.78
	sens.	88.05	85.14	82.58	80.14	64.38	83.85	69.44	65.89	77.43
	accu.	98.14	98.65	94.53	95.04	98.80	99.04	97.42	93.19	96.85
GeoGGVF	spec.	100	100	99.26	99.96	100	99.98	99.59	99.15	99.74
	sens.	87.17	81.24	81.97	78.51	62.93	82.60	86.80	71.38	79.08
	accu.	98.01	98.31	**98.41**	94.74	98.75	**98.98**	**98.55**	94.02	97.47
MAC	spec.	98.59	99.26	95.03	98.01	99.94	98.92	96.37	96.40	97.82
	sens.	97.78	95.17	96.73	92.89	89.31	97.50	98.78	98.22	95.80
	accu.	**98.47**	**98.89**	95.51	**96.76**	**99.58**	98.84	96.56	**96.74**	**97.67**

3 MASS LESION SEGMENTATION

We test these four edge based active contour models to segment lesions in a set of mammogram images. These mass lesion images are also hand labeled so that quantitative analysis can be carried out. Fig. 1 provides an example of mass lesion segmentation using the MAC model. The lesion boundaries are largely diffused. Note the initial contour crosses the region boundary and only sits on the edge of the lesion boundary, which can happen when using automatic lesion detection. This kind of initialization is very challenging for edge based active contour models. The MAC contour did not collapse itself but converged reasonably. None of the other techniques can achieve such result with this difficult initialization. This initialization independence ability of the MAC model makes it particularly suitable for automatic lesion detection and segmentation. Lesion detection algorithms may not be able to find the center of the lesion and often have little knowledge of the shape of the lesion region which makes it very difficult to place the initial contours in the way that is necessary for GGVF or GeoGGVF to

successfully converge. MAC, on the hand, provides great flexibility and robustness.

More examples are given in Fig. 2. The geodesic, GGVF and GeoGGVF had to be carefully initialized, whileas the MAC achieved slightly better results even without dedicated initialization. The quantitative results are shown in Table 1. GGVF, GeoGGVF and MAC all performed reasonably well, except the geodesic snake. MAC generally outperformed the rest.

Overall, we found that MAC's ability to handle difficult initialization provided superior performance. The MAC model showed great potential in automatic lesion detection and segmentation. The shape information and other feature extracted from the segmentation can be passed on for further automatic analysis. This means the whole lesion analysis process can be automated without human intervention, which can improve throughput and may reduce the possibility of false negative since more data can be processed.

4 CONCLUSION

We compared four important edge based active contour model for mass lesion segmentation. This preliminary study on real world mass lesion mammogram image data showed significant improvement in initialization invariancy and convergence capability of the MAC model compared to other advanced edges based methods.

References

[1] V. Caselles, F. Catte, T. Coll, and F. Dibos. A geometric model for active contours. *Numerische Mathematik*, 66(1):1–31, 1993.

[2] D. Guliato, R. Rangayyan, and W. Carnielli. Segmentation of breast tumors in mammograms by fuzzy region growing. In *EMBC*, pages 1002–1005, 2005.

[3] M. Hejaz and Y. Ho. Automated detection of tumors in mammograms using two segments for classification. In *Pacific-Rim Conference on Multimedia*, pages 910–921, 2005.

[4] M. Kupinski and M. Giger. Automated seeded lesion segmentation on digital mammograms. *IEEE T-MI*, 17(4):510–517, 1998.

[5] K. Lee. Segmentation of mammography images using kohonen self-organizing feature maps. In *Midwest Artificial Intelligence and Cognitive Science Conference*, pages 41–46, 1997.

[6] H. Li, M. Kallergi, L. Clarke, and V. Jain. Markov random field for tumor detection in digital mammography. *IEEE T-MI*, 14:565–576, 1995.

[7] N. Paragios, O. Mellina-Gottardo, and V. Ramesh. Gradient vector flow geometric active contours. *IEEE T-PAMI*, 26(3):402–407, 2004.

[8] G. Rad and M. Kashanian. Extraction of the breast cancer tumor in mammograms using genetic active contour. In *Biomed. and Pharmac. Eng.*, pages 30–33, 2006.

[9] M. Sameti and R. Ward. A fuzzy segmentation algorithm for mammogram partitioning. In K. Doi, editor, *Digital Mammography*, pages 471–474. Elsevier, Amsterdam, the Netherlands, 1996.

[10] V. Santos, H. Schiabel, C. Góes, and Benatti. A segmentation technique to detect masses in dense breast digitized mammograms. *J. Digital Imaging*, 15(1):210–213, 2002.

[11] M. Xiao, S. Xia, and S. Wang. Geometric active contour model with color and intensity priors for medical image segmentation. In *EMBC*, pages 6496–6499, 2005.

[12] X. Xie and M. Mirmehdi. MAC: Magnetostatic active contour. *IEEE T-PAMI*, 30(4):636–646, 2008.

[13] C. Xu and J. Prince. Generalized gradient vector flow external forces for active contours. *Signal Processing*, 71(2):131–139, 1998.

[14] R. Yapa and K. Harada. Breast skin-line estimation and breast segmentation in mammograms using fast-marching method. *J. Bio., Biomed., Med. Scis.*, 3(1):54–62, 2008.